The serine-threonine kinase LKB1 is essential for survival under energetic stress in zebrafish

Yme U. van der Velden[a], Liqin Wang[a], John Zevenhoven[a], Ellen van Rooijen[b,c], Maarten van Lohuizen[a], Rachel H. Giles[c,d], Hans Clevers[b], and Anna-Pavlina G. Haramis[a,1]

[a]Department of Molecular Genetics, Netherlands Cancer Institute, 1066 CX, Amsterdam, The Netherlands; [b]Hubrecht Institute, 3584 CT, Utrecht, The Netherlands; and Departments of [c]Medical Oncology and [d]Nephrology, University Medical Center, 3584 CX, Utrecht, The Netherlands

Edited by Ed Harlow, Harvard Medical School, Boston, MA, and approved February 8, 2011 (received for review July 15, 2010)

Mutations in the serine-threonine kinase (LKB1) lead to a gastrointestinal hamartomatous polyposis disorder with increased predisposition to cancer (Peutz–Jeghers syndrome). LKB1 has many targets, including the AMP-activated protein kinase (AMPK) that is phosphorylated under low-energy conditions. AMPK phosphorylation in turn, affects several processes, including inhibition of the target of rapamycin (TOR) pathway, and leads to proliferation inhibition. To gain insight into how LKB1 mediates its effects during development, we generated zebrafish mutants in the single LKB1 ortholog. We show that in zebrafish lkb1 is dispensable for embryonic survival but becomes essential under conditions of energetic stress. After yolk absorption, lkb1 mutants rapidly exhaust their energy resources and die prematurely from starvation. Notably, intestinal epithelial cells were polarized properly in the lkb1 mutants. We show that attenuation of metabolic rate in lkb1 mutants, either by application of the TOR inhibitor rapamycin or by crossing with von Hippel–Lindau (vhl) mutant fish (in which constitutive hypoxia signaling results in reduced metabolic rate), suppresses key aspects of the lkb1 phenotype. Thus, we demonstrate a critical role for LKB1 in regulating energy homeostasis at the whole-organism level in a vertebrate. Zebrafish models of Lkb1 inactivation could provide a platform for chemical genetic screens to identify compounds that target accelerated metabolism, a key feature of tumor cells.

Inactivating mutations in the serine-threonine kinase [LKB1, also known as "serine/threonine kinase 11" (STK11)] cause the cancer-predisposition syndrome Peutz–Jeghers syndrome (PJS) (1). PJS is an autosomal dominant disorder that is characterized by multiple hamartomas of the gastrointestinal tract and abnormal pigmentation of the mucus membranes (2). PJS patients are prone to develop cancer in the gastrointestinal tract and other types of tumors (3). Furthermore, somatic mutations in *LKB1* have been recently identified in ~30% of lung adenocarcinomas (4) and have been identified as a somatic recurrent mutation in endometrial cancer (5).

An important role in establishing cell polarity has been demonstrated for LKB1 (6). Additionally, LKB1 phosphorylates and activates AMP-activated protein kinase (AMPK) as well as 12 related kinases (7, 8). Because AMPK acts as a central energy checkpoint in the cell (9), these findings linked LKB1 signaling to energy metabolism control. Upon energetic stress, LKB1 phosphorylates and activates AMPK that subsequently phosphorylates tuberous sclerosis complex component 1 (TSC1) and 2 (TSC2). This cascade leads to inhibition of the mammalian target of rapamycin (mTOR) signaling pathway with subsequent suppression of protein synthesis and translation, the major energy-consuming processes in the cell.

Although several LKB1 substrates have been identified, it still is not clear how LKB1 exerts its tumor-suppressor activity. The study of mutations in *lkb1* in several model organisms has led to the proposal that LKB1 functions often are cell type-specific and context-dependent. LKB1 was identified originally as part of the partitioning-defective (PAR) proteins that control polarity in *Caenorhabditis elegans* (10). However, recent analysis showed that *C. elegans lkb1* mutants exhibit metabolic defects (11). *Drosophila lkb1* mutants exhibit polarity defects (12). Homozygous deletion of *Lkb1* in mouse is lethal (13), and tissue-specific inactivation of *Lkb1* in several mouse tissues does not lead to polarity defects except in the pancreas (14, 15). To investigate the effects of homozygous loss of function of *lkb1* during development, energy homeostasis, and physiology in vertebrates, we turned to the zebrafish.

lkb1-mutant zebrafish survive gastrulation, unlike their mouse counterparts. We show that *lkb1* is dispensable for embryonic development while the embryo consumes nutrients from the yolk. However, as soon as the yolk is absorbed, the *lkb1* mutants cannot adapt their metabolism, deteriorate rapidly, and die 7 or 8 days postfertilization (dpf). We observe hallmarks of a starvation response in *lkb1* mutants, such as premature depletion of liver glycogen and precocious lipid accumulation in the liver (hepatic steatosis). The *lkb1* mutants exhibit an accelerated metabolic rate, exhaust their energy resources abnormally early, and die from organ failure caused by starvation.

Results and Discussion

Generation of *lkb1*-Mutant Zebrafish. To study the effects of the loss of *lkb1* in zebrafish development, we screened a library of *N*-ethyl-*N*-nitrosourea (ENU)-mutagenized zebrafish by TILLING (16) and identified two independent lines carrying germline nonsense mutations in zebrafish *lkb1*. Both mutations are nucleotide substitutions resulting in premature stop codons in the kinase domain (Fig. S1 *A* and *B*). The mutations correspond to position Y246 and Y261 in human LKB1 (Y245× and Y260×). Notably, the Y246× mutation also has been found in human Peutz–Jeghers patients (17). We studied the *lkb1* mRNA expression pattern during embryonic development by whole-mount in situ hybridization. *Lkb1* mRNA was maternally deposited, and expression was uniform across the embryo during the first 2 d of development. At 3 dpf, we detected strong *lkb1* expression in the head region in WT larvae (Fig. 1*A*). *Lkb1* mRNA expression was severely reduced in *lkb1* mutants, indicating nonsense-mediated decay of the mutant mRNA. To assess whether any remaining Lkb1 was functional, we addressed AMPK phosphorylation in response to anoxia induced by potassium cyanide (KCN) treatment (18). We treated WT and *lkb1*-mutant embryos at 3 dpf with KCN and assessed phosphorylation of AMPK and its downstream substrate acetyl CoA carboxylase (ACC). KCN treatment led to AMPK and ACC phosphorylation in WT embryos, but this response was severely impaired in *lkb1* mutants (Fig. 1*B*). These data indicate that the mutation is a functional null.

Author contributions: A.-P.G.H. designed research; Y.U.v.d.V., L.W., and J.Z. performed research; E.v.R. and R.H.G. contributed new reagents/analytic tools; Y.U.v.d.V., M.v.L., H.C., and A.-P.G.H. analyzed data; and A.-P.G.H. wrote the paper.

The authors declare no conflict of interest.

This article is a PNAS Direct Submission.

Freely available online through the PNAS open access option.

[1]To whom correspondence should be addressed. E-mail: a.haramis@nki.nl.

This article contains supporting information online at www.pnas.org/lookup/suppl/doi:10.1073/pnas.1010210108/-/DCSupplemental.

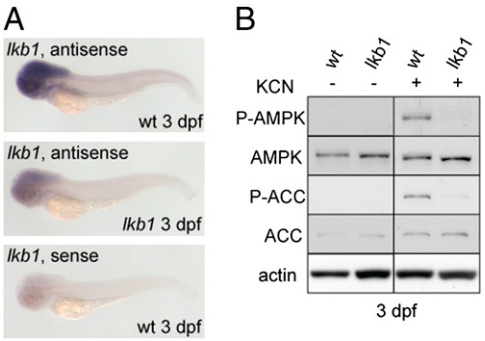

Fig. 1. Characterization of zebrafish *lkb1* mutations. (*A*) Whole-mount in situ hybridizations show decreased *lkb1* mRNA expression in 3-dpf *lkb1*-mutant larvae. (*B*) Western blot analysis of AMPK and ACC upon KCN treatment. KCN treatment results in activation of the AMPK pathway in 3-dpf WT larvae but not in 3-dpf *lkb1*-mutant larvae.

Lkb1 Is Dispensable for Embryonic Survival in Zebrafish. *Lkb1* mutant embryos were indistinguishable from WT siblings for the first 5 d of development. However, at 7 dpf, *lkb1* mutants were emaciated, displayed an abrupt loss of intestinal folding, and had a small, dark liver (Fig. 2). The phenotype was identical for both mutations, and transheterozygote animals demonstrated no allelic complementation. The flattened intestinal epithelia and a dark liver also were observed in WT larvae after prolonged food deprivation (at 11 dpf; Fig. 2 *E* and *F*). The *lkb1* mutants died at 7–8 dpf, whereas WT larvae can survive without food for up to 2 wk. The abrupt loss of intestinal folding in the *lkb1* mutants and the reported role of LKB1 in controlling epithelial polarity prompted us to investigate whether intestinal epithelial cells were polarized properly in *lkb1* mutants.

No Intestinal Polarity Defects in *lkb1* Mutants. The intestinal epithelium initiates folding at around 3–4 dpf in WT embryos, and extensive folding occurs at subsequent developmental stages (19). In *lkb1* mutants, the intestinal epithelium initiated folding normally, and at 5 dpf the villi were visible. However, at 7 dpf an abrupt loss of folding characterized a flattened intestinal epithelium. Sections along the intestinal tract of WT and mutant larvae

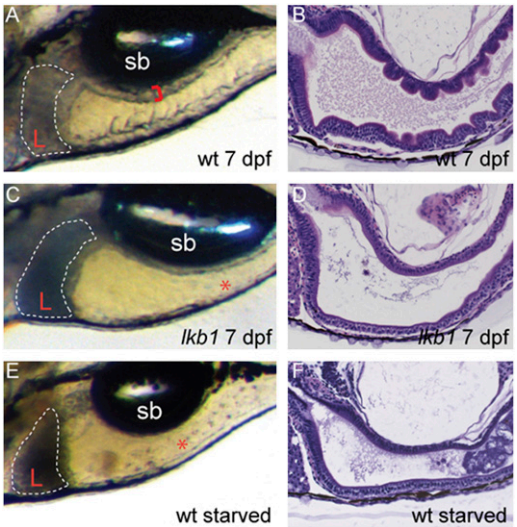

Fig. 2. The intestinal architecture of *lkb1* mutants resembles that of starved WT larvae. (*A*, *C*, and *E*) High-power images depicting the liver and intestine of live larvae of the indicated genotypes; anterior is to the left. Red brackets demarcate the thickness of the intestinal wall, and livers are outlined. At 7 dpf, *lkb1*-mutant larvae (*C*) exhibit a small, dark liver (L) and flattened intestine (asterisk), as do starved 11-dpf WT larvae (*E*). (*B*, *D*, and *F*) H&E staining of sagittal sections of the intestine. Note loss of intestinal folding in 7-dpf *lkb1*- mutant larvae and in starved WT larvae. Sb, swim bladder.

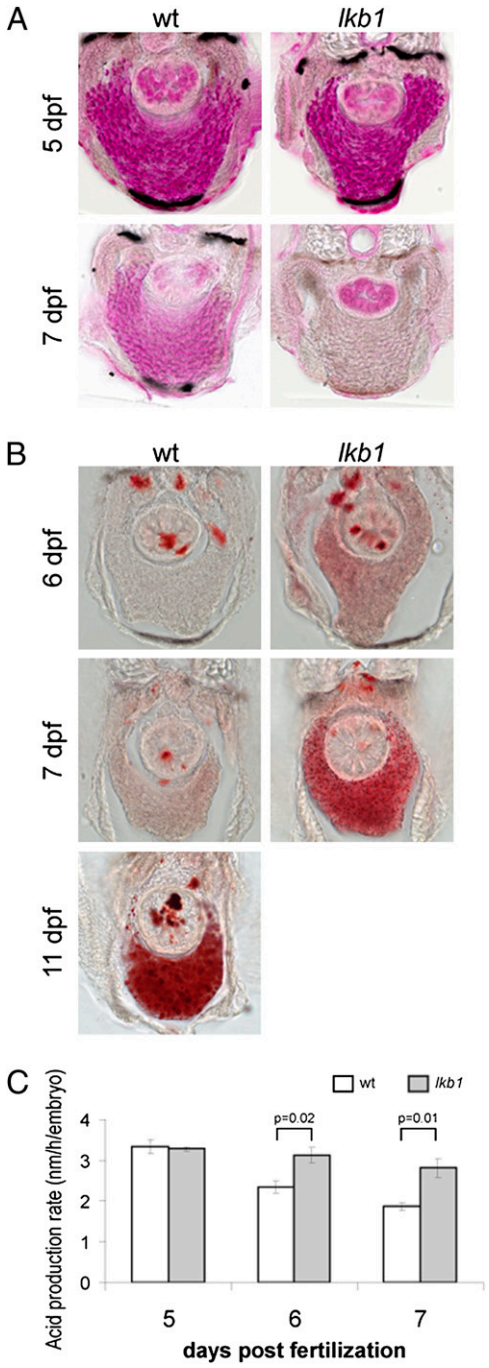

Fig. 3. *lkb1* mutants exhibit hallmarks of response to starvation and high metabolic rate. (*A*) Transverse vibratome sections of PAS-stained WT and *lkb1*-mutant livers at 5 and 7 dpf. At 7 dpf the WT liver still contains a moderate amount of glycogen, but glycogen is depleted in the *lkb1*-mutant liver. (*B*) Transverse vibratome sections of ORO-stained WT and *lkb1*-mutant livers on days indicated. Note strong lipid accumulation in the *lkb1*-mutnt liver at 7 dpf and in starved WT liver at 11 dpf. (*C*) *Lkb1* mutants exhibit high metabolic rate. Histograms depict acid production rates of WT and *lkb1*-mutant larvae at different days of development. The rate of acid production correlates with metabolic rate and was calculated as described in *SI Materials and Methods*.

harvested at 5 and 7 dpf were stained with polarity markers. We did not observe any polarity defects in the intestine of the *lkb1*-mutant larvae. Specifically, the apical markers atypical PKC (aPKC) and F-actin were expressed at normal levels and were localized correctly (Fig. S2 *A–D*). Similarly, staining with β-catenin, E-cadherin, and NA^+/K^+-ATPase revealed normal basolateral localization (Fig. S2 *E–J*). Transmission electron microscopy confirmed normal distribution and morphology of tight junctions and the presence of an apical brush border in the intestinal cells of the *lkb1* mutants (Fig. S3). These results showed that epithelial cell polarity is intact in zebrafish *lkb1* mutants, and the observed phenotype must be attributed to other functions of *lkb1*.

Lkb1 Mutants Resemble Starved WT Larvae. We observed that 7-dpf *lkb1*-mutant larvae phenotypically resemble starving WT animals at 11 dpf. We also noted that *lkb1* mutants do not feed at 5 dpf as expected for WT larvae. We established that lack of feeding was not caused by any structural abnormalities in the jaw or any occlusions in the digestive tract that would prevent *lkb1* mutants from eating. We showed that *lkb1* mutants were capable of ingestion and digestion using *N*-{[6-(2,4-dinitrophenyl)amino]hexanoyl}-1-palmitoyl-2- BODIPY-FL-pentanoyl-*sn*-glycero-3-phosphoethanolamine (PED6), a phospholipase A2 (PLA2) substrate that exhibits increased fluorescence upon cleavage by PLA2 in the intestine. In *lkb1*-mutant larvae, fluorescence in both intestinal lumen and gall bladder was detected at levels equivalent to those in WT larvae (Fig. S4). These results show that *lkb1* mutants are capable of ingestion and digestion but do not feed and suggested a failure to sense energy stress.

Lkb1 Mutants Exhibit Accelerated Energy Depletion and High Metabolic Rate. One of the major LKB1 substrates is AMPK, a critical energy "checkpoint." The fact that the *lkb1* mutants morphologically resemble starving WT animals prompted us to investigate whether the *lkb1* mutants experience prematurely severe energetic stress. We first addressed glycogen consumption. Zebrafish (like other vertebrates) consume glycogen stored in the liver to generate energy. The zebrafish liver contains high amounts of glycogen that is used gradually during the first few days of development (20). Glycogen content of the liver was assessed by periodic acid-Schiff (PAS) staining before and after yolk absorption (5 and 7 dpf, respectively). At 5 dpf, high amounts of glycogen are detected in the liver of WT and *lkb1*-mutant larvae (Fig. 3*A*). In contrast, at 7 dpf the *lkb1* livers already were depleted of glycogen, whereas the WT liver still contained a moderate amount of glycogen (Fig. 3*A*). These results demonstrated premature glycogen depletion from the liver of *lkb1*-mutant larvae.

Starvation induces accumulation of triglycerides and lipids in the liver because of the transport of free fatty acids from peripheral adipose tissue to the liver (21). These lipids can be visualized by staining with the Oil Red O (ORO) dye. ORO staining of WT and *lkb1*-mutant larvae revealed increased lipid accumulation in the liver (hepatic steatosis) of *lkb1* mutants at 7 dpf (Fig. 3*B*). Starved WT larvae at 11 dpf also showed a high degree of hepatic steatosis (Fig. 3*B*). Thus, the *lkb1*-mutant larvae exhibit a response to starvation long before WT larvae do, suggesting accelerated exhaustion of energy reserves. To measure this process, we performed a whole-animal colorimetric assay measuring metabolic rate in zebrafish (22). This assay is based on the direct correlation of acid production with metabolic rate. We found that although the *lkb1*-mutant larvae had metabolic rate similar to that of WT larvae for the first 5 d of development, they had an increased metabolic rate starting at 6 dpf, and at 7 dpf the exacerbation was more pronounced (Fig. 3*C*). We concluded that *lkb1*-mutant zebrafish exhibit accelerated morphological and cellular hallmarks of starvation. We next examined whether *lkb1* mutants also display a response to starvation at the molecular level.

Lkb1 Mutants Display a Response to Starvation at the Molecular Level. Under energetic stress, AMPK phosphorylation triggers a signaling cascade to enable an organism to cope with limited

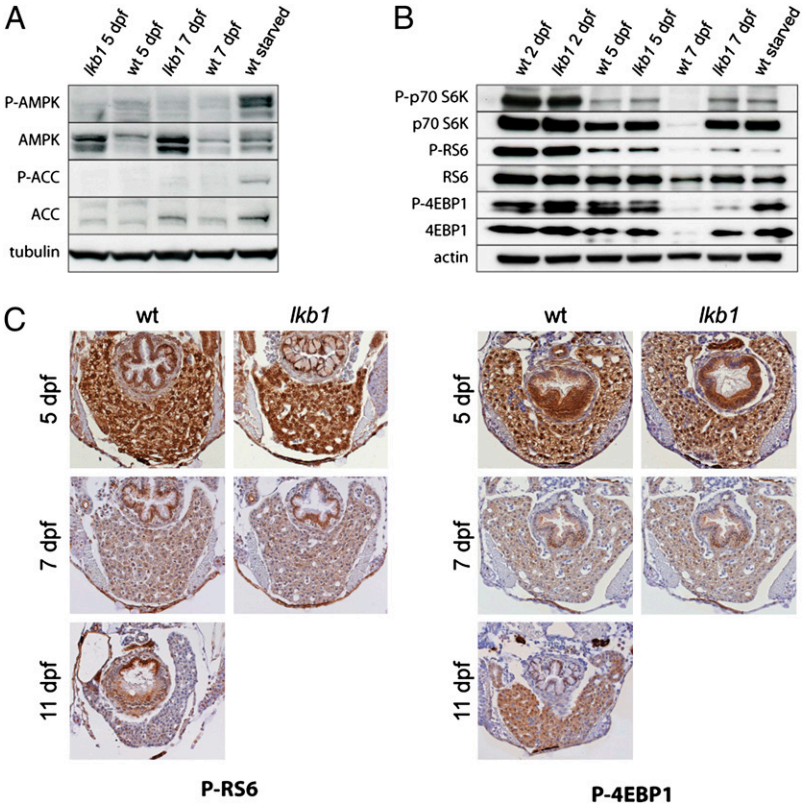

Fig. 4. The zebrafish TOR (zTOR) pathway activity in *lkb1* mutants resembles that in starved WT larvae. (*A*) Western blot analysis with antibodies against phospho-AMPK and phospho-ACC of total protein lysates from embryos at the indicated days and genotypes. AMPK and ACC are not phosphorylated in WT or *lkb1*-mutant larvae at 5 or 7 dpf. Prolonged fasting induces phosphorylation of AMPK and ACC in 11-dpf WT larvae. Elevated expression of AMPK in 7-dpf *lkb1*-mutant larvae is detected. (*B*) Western blot analysis using anti–phospho-p70S6K, anti-p70S6K, anti–phospho-4EBP1, anti-4EBP1, anti–phospho-RS6, and anti-RS6 antibodies of total protein lysates from embryos at the indicated days and genotypes. (*C*) Sections of livers obtained from WT and *lkb1*-mutant embryos at the indicated days stained with anti–phospho-RS6 and anti–phospho-4EBP1.

nutrient supply (9). We assessed the levels of AMPK and its phosphorylation in WT and *lkb1*-mutant larvae at 5 and 7 dpf and in starved WT larvae at 11 dpf. As expected, AMPK was not phosphorylated in *lkb1*-mutant larvae at any point. AMPK was not phosphorylated in WT larvae at 7 dpf either, indicating that at 7 dpf any energetic stress in WT larvae is not sufficient to induce detectable phosphorylation of AMPK. Only prolonged food deprivation led to high levels of AMPK and ACC phosphorylation in starved WT larvae (at 11 dpf) (Fig. 4*A*).

These data suggest that the observed down-regulation of metabolic rate in WT larvae is mediated by additional mechanisms and that the inability to activate AMPK is not the primary reason for the rapid deterioration of *lkb1* fish once the yolk is consumed. Interestingly, total levels of AMPK were increased in *lkb1*-mutant larvae at 7 dpf. This finding suggested that LKB1 function is implicated in the turnover of the AMPK pool.

We next investigated the status of the TOR pathway in *lkb1* mutants. We evaluated the phosphorylation status of ribosomal p70S6 kinase (p70S6K), ribosomal S6 protein (RS6), and factor 4E binding protein 1 (4EBP1), well-established effectors of TOR signaling (23). TOR activity exhibited a dynamic pattern of regulation during development. p70S6K, RS6, and 4EBP1 were highly expressed and phosphorylated at 2 dpf in both WT and *lkb1*-mutant larvae, concomitant with rapid growth and organ expansion (Fig. 4*B*). During the course of subsequent development (5 dpf), the activity of the TOR complex was down-regulated as judged by lower levels of p70S6K, RS6, and, to a lesser extent, 4EBP1 phosphorylation. Presumably, energetic demand following organogenesis is diminished. In 7-dpf WT larvae, we observed remarkable down-regulation of p70S6K and 4EBP1 total levels. In *lkb1* mutants at 7 dpf we observed high expression of p70S6K and 4EBP1 accompanied by moderate levels of phosphorylation (Fig. 4*B*). Prolonged fasting induced reexpression and phosphorylation of p70S6K and 4EBP1 in 11-dpf WT larvae. Thus, the *lkb1* mutants displayed a p70S6K signaling status identical to that in starved WT larvae, whereas phosphorylation of 4EBP1 was higher in starved WT larvae. We next sought to determine regulation of these markers in a time- and organ-specific manner. Immunohistochemistry (IHC) on larvae with antibodies specific to phospho-RS6 and phospho-4EBP1 showed that expression was strong in the liver (Fig. 4*C*) and intestine (Fig. S5) of 5-dpf WT and *lkb1*-mutant larvae. Expression of these markers was weaker in both WT and *lkb1*-mutant larvae at 7 dpf. Consistent with the Western blot results, phospho-4EBP1 expression was increased in the liver of starved WT animals (Fig. 4*C*). We noted that although phospho-RS6 and phospho-4EBP1 expression were regulated over time in the liver and intestine, expression of these markers in the pancreas remained strong throughout development (Fig. S5). Interestingly, we observed that TOR activity is high in starved WT animals despite significant phosphorylation of AMPK at this stage. It is plausible that under severe energetic stress other pathways (in addition to or independent of AMPK signaling) regulate TOR activity. These results showed that the *lkb1* mutants display a status similar to starved WT with respect to TOR activity.

It was reported that treatment with rapamycin, a specific TOR inhibitor (24), lowers metabolism in fish (25). To investigate the effects of rapamycin treatment in the *lkb1* phenotype, we treated *lkb1*-mutant larvae from fertilization onwards. Rapamycin treatment initiated at this very early stage prolonged survival of *lkb1* mutants. At 7 dpf, treated *lkb1*-mutant larvae did not manifest the *lkb1* phenotype (Fig. S6*B*). However, at 10 dpf the *lkb1*-mutant larvae exhibited a dark liver and flattened intestine (Fig. S6*C*). This result showed that pharmacological retardation of metabolism leads to prolonged survival of the *lkb1* mutants, but rapamycin treatment is not sufficient to rescue the *lkb1* phenotype.

Differential Regulation of IGF and PI3K Signaling in *lkb1* Mutants. It was shown recently that starvation in several models leads to reduction of insulin-like growth factor (IGF) and up-regulation of the expression of the inhibitory molecule IGF-binding protein 1 (IGFBP1) (21, 26). We studied *igfbp1* expression in *lkb1* mutants by in situ hybridization. In 7-dpf WT embryos *igfbp* is expressed exclusively in the liver. In *lkb1* mutants, *igfbp1* expression was high in the liver and also was found in the intestine (Fig. S7*B*), as observed in 11-dpf starved WT larvae (Fig. S7*C*). IGF signaling leads to PI3K activation and subsequent activation of TOR and p70S6K. A feedback loop also exists in which phosphorylated p70S6K in turn leads to inhibition of PI3K signaling (27). The observed p70S6K up-regulation in *lkb1* mutants prompted us to address the status of PI3K signaling.

Activation of PI3K signaling by growth factors leads to phosphorylation and activation of protein kinase B (PKB)/AKT. AKT in turn phosphorylates and subsequently inactivates TSC2, an inhibitor of mTOR (23). We evaluated the status of phosphorylated AKT at different time points in WT and *lkb1*-mutant larvae by IHC. Strong phospho-AKT expression was detected in the liver of WT and *lkb1*-mutant larvae at 5 dpf (Fig. 5*A*). In contrast, phospho-AKT was no longer detected in the liver of 7-dpf *lkb1*-mutant larvae, but expression persisted in the liver of 7-dpf WT larvae (Fig. 5*A*). Phospho-AKT expression was barely

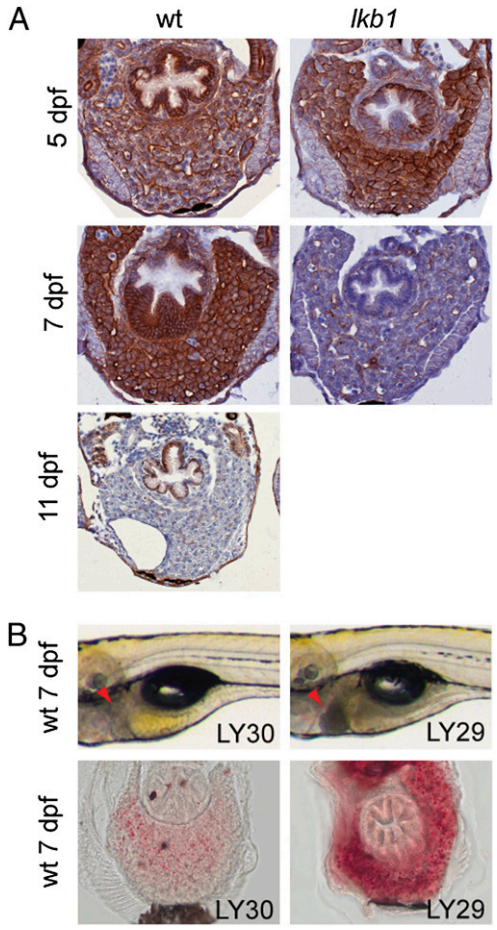

Fig. 5. Deregulation of PI3K signaling in *lkb1* mutants. (*A*) Transverse sections of WT and *lkb1-mutant* livers at indicated days of development stained with an antibody against phospho-AKT. Strong phospho-AKT staining is detected in WT and *lkb1*-mutant livers at 5 dpf. WT liver is strongly stained at 7 dpf, whereas phospho-AKT staining is barely detectable in 7-dpf *lkb1*-mutant liver and in starved WT at 11 dpf. (*B*) Inhibition of PI3K signaling leads to a starvation-like phenotype in WT larvae. WT larvae at 7 dpf treated for 3 d with either LY29 or its inactive analog LY30. LY29 treatment of WT larvae at 4 dpf leads to dark liver (arrowheads) and abnormal hepatic steatosis as revealed by ORO staining. Treatment with the inactive analog LY30 has no effect in the morphology of the larvae.

detectable in the liver of starved WT at 11 dpf (Fig. 5*A*). We obtained an identical pattern of phospho-AKT regulation in the intestine (Fig. S8). These results show that under energetic stress the PI3K pathway is switched off and that in *lkb1* mutants this turning off happens prematurely. We next investigated the effects of PI3K inhibition in WT larvae. Remarkably, we found that treatment of WT larvae with LY294002 (hereafter called "LY29"), an inhibitor of PI3K signaling, phenocopied the *lkb1* liver phenotype in WT larvae. LY29-treated WT animals exhibited a dark liver and abnormal hepatic steatosis at 7 dpf (Fig. 5*B*). Treatment with the inactive analog LY303511 (hereafter "LY30") had no effect on the morphology of the larvae (Fig. 5*B*). These results show that regulation of PI3K signaling is compromised in *lkb1*-mutant larvae and that inhibition of this pathway even after organogenesis is completed can phenocopy certain aspects of the *lkb1* phenotype.

Genetic Interaction Between VHL and LKB1. In several settings, LKB1 inactivation leads to increased sensitivity to stress states including hypoxia; furthermore, hypoxia causes attenuation of metabolism Biochemically, hypoxia leads to activation of the TSC1/2 complex and thus TOR inhibition. To determine whether the *lkb1* mutants are hypoxic, we studied expression of hypoxia-inducible factor 1 subunit alpha (HIF1α) target genes in *lkb1*-mutant larvae. Expression of the HIF1α target genes lactate dehydrogenase a (*ldha*) and NADH dehydrogenase (ubiquinone) 1 α subcomplex 4 (*ndufa4*) was not altered in 7-dpf *lkb1*-mutant larvae compared with WT larvae, indicating that the HIF1α transcription program was not activated in *lkb1*-mutant larvae (Fig. S9). These data appear contradictory to recent studies reporting that *lkb1*-deficient polyps in mice and human PJS patients manifested markedly up-regulated activity of HIF1α and its downstream transcriptional targets (28). However, in that setting HIF1α is a target of increased TOR activity, which is not significantly up-regulated in *lkb1* mutants. To simulate a situation of constitutive hypoxia signaling in the context of *lkb1* homozygous loss of function, we crossed the *lkb1* mutants with von Hippel–Lindau (*vhl*)-mutant fish. The tumor suppressor VHL is an E3 ubiquitin ligase that triggers degradation of HIF1α in the presence of oxygen. Zebrafish *vhl* mutants exhibit a systemic hypoxia response including up-regulation of hypoxia-induced genes (29).

Remarkably, we found that the *lkb1*/*vhl* double mutants morphologically resemble the *vhl* single mutant; no characteristics of the *lkb1* phenotype, such as the flattened intestine and the dark liver, were evident (Fig. 6*A*). Thus, loss of *vhl* suppressed manifestation of the *lkb1* phenotype. The *lkb1*/*vhl* larvae still died at 8 dpf (as do the *vhl* mutants). Our data indicate that the *lkb1* mutants become energy depleted prematurely. The observed suppression of the *lkb1* phenotype in the *lkb1*/*vhl* mutants made us wonder whether metabolic changes induced by *vhl* loss could account for this effect. To address this possibility, we first measured cellular ATP levels of 7-dpf larvae. We found that 7-dpf *lkb1*-mutant larvae indeed exhibit profoundly decreased ATP levels (Fig. 6*B*). Interestingly, 7-dpf *vhl* and *lkb1*/*vhl* mutants also displayed reduced ATP levels compared with WT larvae.

We noted that some 7-dpf *vhl* and *vhl*/*lkb1* mutants had retained some yolk at this late stage. This observation suggested that the *vhl* mutants have a slower metabolic rate. Indeed, we observed that at 3 dpf the *vhl* mutants already displayed a dramatically decreased metabolic rate as compared with WT larvae (Fig. 6*C*). We propose that the rewired overall slow metabolism caused by *vhl* loss is sufficient to suppress the *lkb1* "starvation" phenotype.

We describe here the role of Lkb1 during vertebrate development and physiology. We uncovered that Lkb1 deficiency in zebrafish leads to a broad inability to maintain energy homeostasis at the whole-organism level and that Lkb1 is critically required for the adaptation of energy metabolism in anticipation of scarce nutrient conditions. The *lkb1* mutants fail to down-regulate their metabolism at the transition between endonu-

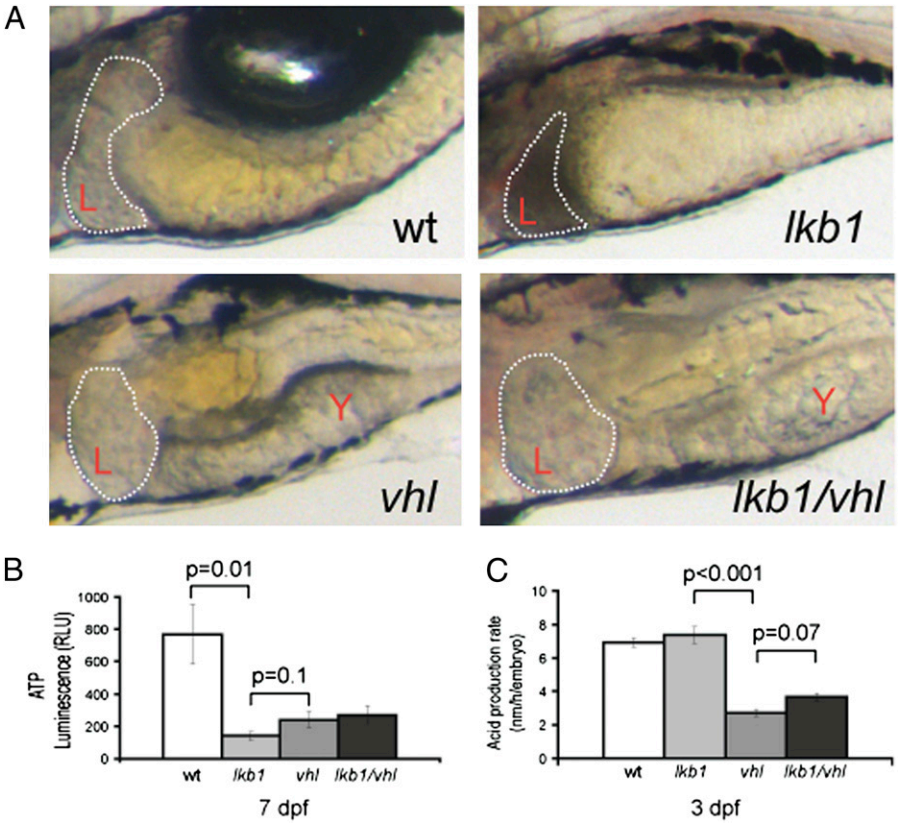

Fig. 6. Loss of *vhl* suppresses manifestation of the *lkb1* phenotype. (*A*) High-power images depicting the liver and intestine of live larvae of the indicated genotypes at 7 dpf; anterior is to the left. Note that some yolk (Y) is still present. The intestine is folded, and the liver is clear in the *lkb1*/*vhl* larva. (*B*) Graph showing ATP levels as measured in relative light units (RLU). The *lkb1* embryos have very low ATP levels; ATP levels are decreased in *vhl* and *lkb1*/*vhl* embryos but are slightly higher than in *lkb1*-mutant embryos. (*C*) Graph representing the metabolic rate of larvae of different genotypes at 3 dpf. The *lkb1*-mutant larvae have an increased metabolic rate as compared with WT larvae. The *vhl* larvae display a dramatically low metabolic rate, and the *lkb1*/*vhl* larvae also display a low metabolic rate.

trition and ectonutrition states; thus, Lkb1 function becomes critically essential once the yolk is consumed. The *lkb1* mutants exhibit hallmarks of a starvation response at the cellular and biochemical level, display profoundly decreased ATP levels, and become energy depleted much sooner than food-deprived WT animals. We do not observe an overt up-regulation of TOR activity in the *lkb1* mutants, and although rapamycin treatment prolongs survival, it fails to rescue the mutant phenotype. LKB1 activates several AMPK-related kinases, some of which also are involved in energy metabolism control, and AMPK regulates cell metabolism through multiple pathways in addition to TOR complex 1 (TORC1). We propose that the apmk-torc1 axis may not be the only or the critical effector of Lkb1-mediated maintenance of whole-organism energy homeostasis in this setting. Indeed, very recently the effects of *Lkb1* inactivation in mouse hematopoietic stem cells were reported (30–32). Although LKB1 is critically required to regulate energy metabolism in mouse hematopoietic stem cells and to maintain their survival, the effects were largely independent of LKB1 regulation of AMPK and TORC1 signaling in this setting (30–32).

We demonstrate that the intestinal epithelial cells in *lkb1* mutants were polarized properly. Despite flattening of the intestinal epithelium in 7-dpf *lkb1* mutants, polarity markers are localized properly and are expressed at levels comparable to those in WT larvae. The *lkb1* intestinal epithelial cells show a normal microvilli network and normal distribution of tight junctions. No malformations in other polarized organs such as the eye were observed, either. The *Drosophila lkb1* mutant exhibits polarity defects (12, 33), but *lkb1* deficiency in mice does not lead to polarity defects with the exception of the pancreas (14, 15). Our data and those of others (34) suggest that in vertebrates the function of LKB1 in polarity may be compensated by other pathways.

Lkb1 in zebrafish is a larval-lethal mutation, and homozygous mutant embryos do not display gross morphological abnormalities during early embryonic development. It is plausible that in fish Lkb1 protein is maternally provided and is sufficient to enable the embryos to complete gastrulation, but we show that any maternal Lkb1 stores are depleted by 3 dpf. This finding is consistent with a recent study reporting the effects of Lkb1 knock down by morpholinos in zebrafish (35). In this study, no gastrulation defects were observed, and the analysis focused on the role of Lkb1 in intestinal differentiation. Our analysis focuses on later larval stages and indicates that the essential function of Lkb1 in zebrafish is to regulate energy metabolism.

We found that Lkb1 has a critical role in the ability to maintain energy homeostasis in response to changing conditions in the environment in zebrafish. The *lkb1*-mutant larvae will serve as valuable tools in chemical genetic screens aimed at identifying compounds that can suppress their high metabolic rate.

Materials and Methods

Zebrafish Strains. Zebrafish were maintained at 28 °C. Fish were cared for in accordance with institutional guidelines and as approved by the Animal Experimentation Committee of the Royal Netherlands Academy of Arts and Sciences. Details of the ENU screening and identification of the mutations are described in *SI Materials and Methods*.

Western Blot Analyses. Larvae were lysed in Brye buffer for 30 min followed by sonication for 5 min. Protein extracts were separated on 4–12% bis-Tris precast gels (NuPAGE) and transferred to Immobilon-P membranes (Amersham Biosciences). Primary antibodies were diluted in PBS with Triton-X (PBT) containing 1% BSA and 4% Western blot blocking reagent (Roche). Primary antibodies used are described in *SI Materials and Methods*.

Metabolic Rate Assay. The metabolic rate assay was performed essentially as described in ref. 22 with some modifications listed in *SI Materials and Methods*.

ACKNOWLEDGMENTS. We thank H. Jansen for electron microscopy analysis, L. Oomen and L. Brooks for confocal microscopy, A. Spaarman, F. van Leeuwen, and A. Perrakis for critical advice on the manuscript, B. Mendelsohn and J. Gitlin for advice on KCN treatment and ATP measurements in fish, and the animal caretakers for excellent care of the fish. This work was funded by Netherlands Organization for Scientific Research Vidi Grants 91756322 (to A.-P.G.H.) and 91766354 (to R.H.G.). R.H.G. also receives funds from EU FP7/2009 SYSCILIA project 241955.

1. Hemminki A, et al. (1998) A serine/threonine kinase gene defective in Peutz-Jeghers syndrome. *Nature* 391:184–187.
2. Jeghers H, McKusick VA, Katz KH (1949) Generalized intestinal polyposis and melanin spots of the oral mucosa, lips and digits; a syndrome of diagnostic significance. *N Engl J Med* 241:993–, illust passim.
3. Giardiello FM, et al. (1987) Increased risk of cancer in the Peutz-Jeghers syndrome. *N Engl J Med* 316:1511–1514.
4. Ji H, et al. (2007) LKB1 modulates lung cancer differentiation and metastasis. *Nature* 448:807–810.
5. Contreras CM, et al. (2008) Loss of Lkb1 provokes highly invasive endometrial adenocarcinomas. *Cancer Res* 68:759–766.
6. Baas AF, et al. (2004) Complete polarization of single intestinal epithelial cells upon activation of LKB1 by STRAD. *Cell* 116:457–466.
7. Shaw RJ, et al. (2004) The tumor suppressor LKB1 kinase directly activates AMP-activated kinase and regulates apoptosis in response to energy stress. *Proc Natl Acad Sci USA* 101:3329–3335.
8. Hawley SA, et al. (2003) Complexes between the LKB1 tumor suppressor, STRAD alpha/beta and MO25 alpha/beta are upstream kinases in the AMP-activated protein kinase cascade. *J Biol* 2:28.1–28.16.
9. Hardie DG (2007) AMP-activated/SNF1 protein kinases: Conserved guardians of cellular energy. *Nat Rev Mol Cell Biol* 8:774–785.
10. Wodarz A (2002) Establishing cell polarity in development. *Nat Cell Biol* 4:E39–E44.
11. Narbonne P, Roy R (2009) *Caenorhabditis elegans dauers* need LKB1/AMPK to ration lipid reserves and ensure long-term survival. *Nature* 457:210–214.
12. Martin SG, St Johnston D (2003) A role for Drosophila LKB1 in anterior-posterior axis formation and epithelial polarity. *Nature* 421:379–384.
13. Ylikorkala A, et al. (2001) Vascular abnormalities and deregulation of VEGF in Lkb1-deficient mice. *Science* 293:1323–1326.
14. Granot Z, et al. (2009) LKB1 regulates pancreatic beta cell size, polarity, and function. *Cell Metab* 10:296–308.
15. Hezel AF, et al. (2008) Pancreatic LKB1 deletion leads to acinar polarity defects and cystic neoplasms. *Mol Cell Biol* 28:2414–2425.
16. Wienholds E, et al. (2003) Efficient target-selected mutagenesis in zebrafish. *Genome Res* 13:2700–2707.
17. Nakagawa H, et al. (1998) Nine novel germline mutations of STK11 in ten families with Peutz-Jeghers syndrome. *Hum Genet* 103:168–172.
18. Mendelsohn BA, Kassebaum BL, Gitlin JD (2008) The zebrafish embryo as a dynamic model of anoxia tolerance. *Dev Dyn* 237:1780–1788.
19. Horne-Badovinac S, et al. (2001) Positional cloning of heart and soul reveals multiple roles for PKC lambda in zebrafish organogenesis. *Curr Biol* 11:1492–1502.
20. Pack M, et al. (1996) Mutations affecting development of zebrafish digestive organs. *Development* 123:321–328.
21. Lee C, et al. (2010) Reduced levels of IGF-I mediate differential protection of normal and cancer cells in response to fasting and improve chemotherapeutic index. *Cancer Res* 70:1564–1572.
22. Makky K, Duvnjak P, Pramanik K, Ramchandran R, Mayer AN (2008) A whole-animal microplate assay for metabolic rate using zebrafish. *J Biomol Screen* 13:960–967.
23. Inoki K, Li Y, Zhu T, Wu J, Guan KL (2002) TSC2 is phosphorylated and inhibited by Akt and suppresses mTOR signalling. *Nat Cell Biol* 4:648–657.
24. Wullschleger S, Loewith R, Hall MN (2006) TOR signaling in growth and metabolism. *Cell* 124:471–484.
25. Makky K, Tekiela J, Mayer AN (2007) Target of rapamycin (TOR) signaling controls epithelial morphogenesis in the vertebrate intestine. *Dev Biol* 303:501–513.
26. Raffaghello L, et al. (2008) Starvation-dependent differential stress resistance protects normal but not cancer cells against high-dose chemotherapy. *Proc Natl Acad Sci USA* 105:8215–8220.
27. Manning BD (2004) Balancing Akt with S6K: Implications for both metabolic diseases and tumorigenesis. *J Cell Biol* 167:399–403.
28. Shackelford DB, et al. (2009) mTOR and HIF-1alpha-mediated tumor metabolism in an LKB1 mouse model of Peutz-Jeghers syndrome. *Proc Natl Acad Sci USA* 106:11137–11142.
29. van Rooijen E, et al. (2009) Zebrafish mutants in the von Hippel-Lindau tumor suppressor display a hypoxic response and recapitulate key aspects of Chuvash polycythemia. *Blood* 113:6449–6460.
30. Gan B, et al. (2010) Lkb1 regulates quiescence and metabolic homeostasis of haematopoietic stem cells. *Nature* 468:701–704.
31. Gurumurthy S, et al. (2010) The Lkb1 metabolic sensor maintains haematopoietic stem cell survival. *Nature* 468:659–663.
32. Nakada D, Saunders TL, Morrison SJ (2010) Lkb1 regulates cell cycle and energy metabolism in haematopoietic stem cells. *Nature* 468:653–658.
33. Mirouse V, Swick LL, Kazgan N, St Johnston D, Brenman JE (2007) LKB1 and AMPK maintain epithelial cell polarity under energetic stress. *J Cell Biol* 177:387–392.
34. Shackelford DB, Shaw RJ (2009) The LKB1-AMPK pathway: Metabolism and growth control in tumour suppression. *Nat Rev Cancer* 9:563–575.
35. Marshall KE, Tomasini AJ, Makky K, N Kumar S, Mayer AN (2010) Dynamic Lkb1-TORC1 signaling as a possible mechanism for regulating the endoderm-intestine transition. *Dev Dyn* 239:3000–3012.